Articles

Diastereospecific Ion-Pairing Polymerization of Functionalized Alkenes by Metallocene/Lewis Acid Hybrid Catalysts

Yalan Ning and Eugene Y.-X. Chen*

Department of Chemistry, Colorado State University, Fort Collins, Colorado 80523-1872

Received July 25, 2006

ABSTRACT: This work studies the mechanism and application of the novel diastereospecific ion-pairing polymerization (DIPP) effected by a catalyst system comprising chiral zirconocene bis(ester enolate) *rac*-(EBI)-Zr[OC(O^{i}Pr)═CMe$_2$]$_2$ [**1**, EBI = $C_2H_4(Ind)_2$] and 2 equiv of Lewis acid Al(C_6F_5)$_3$. The **1**/2Al(C_6F_5)$_3$ system effectively promotes DIPP of functionalized alkenes such as methyl methacrylate (MMA), producing polymers having various stereoregularities, including isotactic, syndiotactic, and isotactic-*b*-syndiotactic multiblock microstructures, depending on the [monomer]/[catalyst] ratio employed. Our detailed investigations into the polymerization characteristics and kinetics, elementary reactions, characterization and behavior of the isolated key intermediates, as well as temperature and Lewis acid effects have yielded a mechanism for the DIPP of MMA by the **1**/2Al(C_6F_5)$_3$ system. This mechanism consists of four manifolds—isospecific, syndiospecific, anion-monomer exchange, and chain-transfer domains—and satisfactorily explains the formation of various polymer stereomicrostructures under given conditions. The most significant part of this overall mechanism is for the production of the isotactic-*b*-syndiotactic stereomultiblock structure, which is made possible by two pathways that can interconvert diastereospecific propagating manifolds: exchange between the coordinated anion and monomer as well as chain transfer. This unique polymerization technique has also been applied to the copolymerization of MMA with methacrylates having longer alkyl chains, leading to functionalized polymeric materials with tunable properties that are controlled by their stereomicrostructures and nature of the comonomer.

Introduction

Organometallic and polymer chemistry has recently experienced phenomenal scientific and commercial successes in the production of revolutionary polyolefin materials by (co)-polymerization of nonpolar α-olefins with metallocene and related catalysts.[1] An ongoing paradigm shift on utilization of highly active, readily accessible, and highly versatile group 4 metallocene and related complexes for the polymerization of polar functionalized alkenes has paid increasing attention to the polymerization of methacrylates,[2] acrylates,[3] and acrylamides;[4] owing to the catalyst structure diversity and tunability, most of these polymerization systems exhibit a high degree of control over polymer structures (microstructure and architecture). This shift, however, is typically accompanied by a switch of the polymerization mechanism, i.e., from migratory insertion polymerization of α-olefins to coordinative (anionic) addition polymerization of functionalized alkenes.

The resulting functionalized polar vinyl polymers such as poly(methyl methacrylate) P(MMA) have stereogenic centers in the repeating units, and the physical and mechanical properties of these polymers depend largely on their stereochemistry.[5] By virtue of the nature of ligand and metal as well as the stereochemical control mechanism, group 4 metallocene and related complexes have demonstrated their ability to control stereoregulation of the polymerization of methacrylates and acrylamides, leading to production of the polymers having diverse tacticities, including atactic (*at*-), isotactic (*it*-), syndiotactic (*st*-), and isotactic-*b*-syndiotactic (*it*-*b*-*st*) stereoblock (*sb*) microstructures.[2,4] Our particular interest in the production of poly(functionalized alkene)s with various stereomultiblock microstructures rests on a common belief that introduction of new stereomicrostructures to functionalized vinyl polymers will lead to new materials properties and thus potentially new applications; a testament of this belief was nicely demonstrated by past examples such as polypropylene (PP)—both *it*- and *at*-PPs are thermoplastic materials, but *it*-*b*-*at sb*-PP is a particularly useful thermoplastic elastomer.[6] In the case of P(MMA), the stereochemistry adds another dimension to its materials properties: a stereocomplex—by definition, a crystalline polymer complex between a pair of diastereomeric macromolecules—can be formed between highly *it*- and *st*-P(MMA) blends in a typical 1:2 ratio either in the solid state, when annealed, or in suitable solvents.[7] This self-assembled, double-stranded helical complex exhibits enhanced physical and mechanical properties when compared to the individual tactic polymers. Therefore, the production of *it*-*b*-*st sb*-P(MMA)[8] is of great interest because diastereomeric P(MMA) chains in the stereoblock composite become chemically linked, and thus stereocomplex formation of helical structures is expected to be more facile and diverse (e.g., intermolecular vs intramolecular stereocomplex formation).

To this end, we communicated earlier a novel diastereospecific ion-pairing polymerization (DIPP) that produces multi-*it*-*b*-*st sb*-P(MMA).[2n] That initial system employed a catalyst mixture containing chiral zirconocenium methyl cations paired

* Corresponding author. E-mail: eychen@lamar.colostate.edu.

10.1021/ma061687w CCC: $33.50
Published on Web 09/15/2006

with both methyl borate and methyl aluminate anions, e.g., *rac*-(EBI)ZrMe$^+$[MeB(C_6F_5)$_3^-$]$_{0.5}$[MeAl(C_6F_5)$_3^-$]$_{0.5}$, which is generated by activation of *rac*-(EBI)ZrMe$_2$ with a 1:1 ratio of Lewis acids E(C_6F_5)$_3$ (E = B, Al). The polymerization of MMA by such a system was proposed to proceed in a diastereospecific ion-pairing fashion, in which the Zr^+/B^- ion pair produces the *it*-block via the zirconium ester enolate cation and the Zr^+/Al^- ion pair affords the *st*-block via the enolaluminate anion, whereas the exchange of growing diastereomeric polymer chains occurs via a neutral zirconocene bis(ester enolate) intermediate to yield *it-b-st* multiblock P(MMA).

Details of the DIPP mechanism, however, remained unknown before the current work. Additionally, that early system affords only short blocks with an average length of *it*- and *st*-sequences of approximately five. Accordingly, our continued studies of this unique DIPP over the past 3 years have been focused on mechanistic aspects of the polymerization as well as development of the DIPP system with higher efficiency and degree of control over diastereomeric blocks. We recognized that the polymerization by the early system employing the chiral zirconocenium methyl cations paired with mixed methyl borate and methyl aluminate anions commences with slow initiation steps that involve transfers of methyl groups to the activated monomers by the Zr cation and by the Al Lewis acid to generate cationic zirconocenium ester enolate and anionic enolaluminate diastereospecific propagating species; these slow initiation steps hampered our mechanistic studies and also resulted in the formation of ill-controlled polymer products. Subsequently, we reasoned that a new system consisting of the preformed propagating intermediate, zirconocene bis(ester enolate) complex *rac*-(EBI)Zr[OC(O^{i}Pr)=CMe$_2$]$_2$,[2f] and 2 equiv of strongly Lewis acidic alane Al(C_6F_5)$_3$, should form rapidly, in the presence of MMA, the diastereospecific propagating species in a single fast reaction, thus eliminating those slow initiation steps in the earlier system. As a result, the new **1**/2Al(C_6F_5)$_3$ catalyst system should lead to a DIPP process with higher efficiency and enhanced control over polymerization characteristics; equally important is the excellent opportunity, offered by this controlled system, to investigate the kinetics and mechanism of DIPP. With these goals in mind, we present here a full account of our efforts to understand the polymerization control, stereoregulation, active species, kinetics, and mechanism of DIPP, using the **1**/2Al(C_6F_5)$_3$ system for the polymerization and copolymerization of MMA and other alkyl methacrylates under systematically varied conditions.

Experimental Section

Materials and Methods. All syntheses and manipulations of air- and moisture-sensitive materials were carried out in flamed Schlenk-type glassware on a dual-manifold Schlenk line, a high-vacuum line (typically 10^{-5}−10^{-7} Torr), or in an argon or nitrogen-filled glovebox (typically <1.0 ppm oxygen and moisture). NMR-scale reactions (typically in a 0.02 mmol scale in ~0.7 mL of an NMR solvent) were conducted in Teflon-valve-sealed J. Young-type NMR tubes. HPLC grade organic solvents were sparged extensively with nitrogen during filling of the 20 L solvent reservoir and then dried by passage through activated alumina (for THF, Et_2O, and CH_2Cl_2) followed by passage through Q-5-supported copper catalyst (for toluene and hexanes) stainless steel columns. Benzene-d_6 and toluene-d_8 were degassed, dried over sodium/potassium alloy, and filtered before use, whereas $CDCl_3$ and CD_2Cl_2 were degassed and dried over activated Davison 4 Å molecular sieves. NMR spectra were recorded on either a Varian Inova 300 (FT 300 MHz, ^{1}H; 75 MHz, ^{13}C; 282 MHz, ^{19}F) or a Varian Inova 400 spectrometer. Chemical shifts for ^{1}H and ^{13}C spectra were referenced to internal solvent resonances and are reported as ppm relative to tetramethylsilane, whereas ^{19}F NMR spectra were referenced to external $CFCl_3$. Elemental analyses were performed by Desert Analytics, Tucson, AZ.

Methyl methacrylate (MMA), *n*-butyl methacrylate (BMA), and 2-ethylhexyl methacrylate (EHM) were purchased from Aldrich, Alfa Aesar, and TCI America, respectively, and purified by degassing and drying over CaH_2 for 2 days, followed by vacuum distillation; final purification of MMA involved titration with neat tri(*n*-octyl)aluminum to a yellow end point[9] followed by a second vacuum distillation. The purified monomers were stored in brown glass bottles in a −30 °C freezer inside the glovebox. 2,6-Di-*tert*-butyl-4-methylphenol (butylated hydroxytoluene, BHT-H) was purchased from Aldrich Chemical Co. and recrystallized from hexanes prior to use.

Tris(pentafluorophenyl)borane B(C_6F_5)$_3$ was obtained as a research gift from Boulder Scientific Co. and further purified by recrystallization from hexanes at −30 °C. Tris(pentafluorophenyl)-alane Al(C_6F_5)$_3$, as a 0.5 toluene adduct Al(C_6F_5)$_3$·(C_7H_8)$_{0.5}$, was prepared by the reaction of B(C_6F_5)$_3$ and AlMe$_3$ in a 1:3 toluene/hexanes solvent mixture in quantitative yield;[10] this is the modified synthesis based on literature procedures.[11] Although we have experienced no incidents when handling this material, *extra caution should be exercised*, especially when dealing with the unsolvated form, because of its thermal and shock sensitivity. The alane employed in this work is the toluene adduct. The Al(C_6F_5)$_3$·MMA adduct[2w] was prepared by addition of excess MMA to a toluene solution of the alane followed by removal of the volatiles and drying in vacuo; when no isolation is needed, this adduct can be prepared by direct mixing of Al(C_6F_5)$_3$ with MMA. Literature procedures were employed for the preparation of the following compounds and metallocene complexes: MeAl(BHT)$_2$,[12] (EBI)H$_2$ [EBI = C_2H_4-(Ind)$_2$],[13] *rac*-(EBI)Zr(NMe$_2$)$_2$,[14] *rac*-(EBI)ZrMe$_2$,[14] and *rac*-(EBI)-Zr[OC(O^{i}Pr)=CMe$_2$]$_2$ (**1**).[2f]

Isolation of [*rac*-(EBI)Zr(OC(OMe)=C(Me)CH$_2$C(Me$_2$)C-(O^{i}Pr)=O)]$^+$[(C_6F_5)$_3$Al−OMe−Al(C_6F_5)$_3$]$^-$ (2). In an argon-filled glovebox, a 30 mL glass reactor was charged with **1** (30.3 mg, 0.05 mmol), Al(C_6F_5)$_3$·MMA (62.8 mg, 0.10 mmol), and 15 mL of CH_2Cl_2. The resulting yellow solution was stirred for 24 h at ambient temperature, after which the orange-red suspension was filtered. The solvent of the filtrate was removed, and the resulting residue was extensively dried in vacuo, affording 63.3 mg (76%) of complex **2** as an orange-red solid. The cation portion of **2** is identical to the cyclic ester enolate zirconocenium cation that is paired with the methylborate anion, *rac*-(EBI)Zr[OC(OMe)=C(Me)CH$_2$C(Me$_2$)C(O^{i}Pr)=O]$^+$[MeB(C_6F_5)$_3$]$^-$, which was derived from the single MMA addition to *rac*-(EBI)Zr$^+$(THF)[OC(O^{i}Pr)=CMe$_2$][MeB(C_6F_5)$_3$]$^-$ and spectroscopically/analytically (but not structurally) characterized.[2b] Accordingly, single crystals of **2** suitable for X-ray diffraction studies were grown from toluene at −30 °C inside the freezer of the glovebox.

^{1}H NMR (CD_2Cl_2, 21 °C) for **2**: δ 8.06 (d, J = 8.4 Hz, 1H), 7.95 (d, J = 8.4 Hz, 1H), 7.38−7.23 (m, 6H), 6.31 (d, J = 3.3 Hz, 1H), 6.27 (d, J = 3.3 Hz, 1H), 6.23 (d, J = 3.3 Hz, 1H), 5.95 (d, J = 3.0 Hz, 1H), 4.34 (sept, J = 6.4 Hz, 1H, C*H*Me$_2$), 4.12−3.97 (m, 4H, CH_2CH_2), 4.05 (s, br, 3H, AlO*Me*), 3.14 (s, 3H, O*Me*), 2.28 (s, br, 2H, CH_2), 1.52 (s, 3H, =C*Me*), 1.40 (d, J = 6.3 Hz, 3H, CH*Me*$_2$), 1.29 (d, J = 6.3 Hz, 3H, CH*Me*$_2$), 1.26−1.16 (m, 6H, C*Me*$_2$). ^{19}F NMR (CD_2Cl_2, 21 °C): δ −119.36 (d, 12F, *o*-F), −154.19 (t, 6F, *p*-F), −162.17 (m, 12F, *m*-F).

Isolation of *rac*-(EBI)Zr[OC(OMe)=C(Me)CH$_2$C(Me$_2$)C-(O^{i}Pr)=O·Al(C_6F_5)$_3$]$_2$ (3). In an argon-filled glovebox, a 60 mL glass reactor was charged with **1** (12.1 mg, 0.02 mmol), Al(C_6F_5)$_3$·MMA (25.1 mg, 0.04 mmol), and 25 mL of hexanes. The resulting yellow suspension was stirred for 30 min at ambient temperature, after which the reaction mixture was filtered. The filtrate was concentrated under reduced pressure to ~0.5 mL and subsequently cooled to −30 °C inside the freezer of the glovebox over 2 h. The supernatant was quickly decanted, and the solid collected was extensively dried in vacuo to give 28.0 mg (76%) of complex **3** as a yellow power. Anal. Calcd for $C_{80}H_{58}Al_2F_{30}O_8Zr$: C, 51.59; H, 3.14. Found: C, 51.42; H, 2.84.

^{1}H NMR (C_6D_6, 21 °C) for **3**: δ 7.28 (d, J = 8.4 Hz, 2H), 7.06 (d, J = 8.4 Hz, 2H), 6.90−6.85 (m, 4H), 5.99 (d, J = 3.0 Hz, 2H), 5.80 (d, J = 3.0 Hz, 2H), 5.19 (sept, J = 6.4 Hz, 2H, C*H*Me$_2$), 3.23 and 3.10 (m, 4H, CH_2CH_2), 2.99 (s, 6H, O*Me*), 2.31 (q_{AB}, 4H, CH_2), 1.28 (s, 6H, =C*Me*), 1.12 (d, J = 6.0 Hz, 12H, CH*Me*$_2$), 0.86 (m, 12H, C*Me*$_2$). ^{13}C NMR (C_6D_6, 21°C): δ 189.0 [*C*(O^{i}Pr)=O], 158.35 (O*C*(OMe)=), 150.33 (d, $^1J_{C-F}$ = 211.0 Hz, C_6F_5), 142.06 (d, $^1J_{C-F}$ = 251.6 Hz, C_6F_5), 137.29 (d, $^1J_{C-F}$ = 251.5 Hz, C_6F_5), 132.14, 125.78, 124.81, 123.73, 122.71, 122.39, 121.08, 115.18, 103.02 (a total of 9 resonances for the indenyl carbons), 79.91 (=*C*Me$_2$), 78.22 (O*C*HMe$_2$), 54.35 (O*C*H$_3$), 45.90 (*C*H$_2$), 41.79 (*C*Me$_2$), 29.09 (*C*H$_2$*C*H$_2$), 24.45 (OCH*Me*$_2$), 23.56 (OCH*Me*$_2$), 20.65 (C*Me*$_2$), 17.36 (=C*Me*). ^{19}F NMR (C_6D_6, 21 °C): δ −122.90 (d, 12F, *o*-F), −152.07 (t, 6F, *p*-F), −161.20 (m, 12F, *m*-F).

Generation of *rac*-(EBI)Zr[OC(OMe)=C(Me)CH$_2$C(Me$_2$)C-(O^{i}Pr)=O·Al(C$_6$F$_5$)$_3$] [OC(O^{i}Pr)=CMe$_2$] (4). In an argon-filled glovebox, a 60 mL glass reactor was charged with **1** (18.2 mg, 0.03 mmol), Al(C_6F_5)$_3$·MMA (18.8 mg, 0.03 mmol), and 30 mL of hexanes. The resulting yellow suspension was stirred for 10 min at ambient temperature, after which ^{1}H NMR of an aliquot showed an incomplete consumption of **1**. Accordingly, a second portion of Al(C_6F_5)$_3$·MMA (0.01 mmol) was added, and the mixture was stirred for another 20 min. The reaction mixture was filtered, and the filtrate was concentrated under reduced pressure to ∼2 mL. The concentrated filtrate was left inside a −30 °C freezer of the glovebox. The supernatant was quickly decanted, and the solid collected was extensively dried in vacuo to give 27.8 mg of the product as a yellow solid. NMR spectra of the product showed formation of the title complex **4**, but accompanied by ∼40% of complex **3** (i.e., the 1:2 ratio reaction product); repeated attempts to separate them by recrystallization were unsuccessful.

^{1}H NMR (C_6D_6, 21 °C) for **4**: δ 7.35 (m, 2H), 7.25−7.05 (m, 3H), 6.89 (m, 3H), 6.39 (d, J = 3.0 Hz, 1H), 6.05 (d, J = 3.0 Hz, 1H), 5.96 (d, J = 3.0 Hz, 1H), 5.87 (d, J = 3.0 Hz, 1H), 5.19 (sept, J = 6.4 Hz, 1H, C*H*Me$_2$), 3.65 (sept, J = 6.4 Hz, 1H, C*H*Me$_2$), 3.31 and 3.16 (m, 4H, CH_2CH_2), 2.97 (s, 3H, O*Me*), 2.34 (q_{AB}, 2H, CH_2), 1.73 and 1.44 (s, 3H, =C*Me*$_2$), 1.31 (s, 3H, =C*Me*), 1.23 (d, J = 6.3 Hz, 3H, CH*Me*$_2$), 1.16 (d, J = 6.0 Hz, 6H, CH*Me*$_2$), 1.07 (d, J = 6.3 Hz, 3H, CH*Me*$_2$), 0.89 (m, 6H, C*Me*$_2$). ^{19}F NMR (C_6D_6, 21 °C): δ −122.87 (d, 12F, *o*-F), −152.14 (t, 6F, *p*-F), −161.25 (m, 12F, *m*-F).

Isolation of [*rac*-(EBI)Zr(OC(O^{i}Pr)=CMe$_2$)]$^+$[O=C(O^{i}Pr)C-(Me$_2$)B(C$_6$F$_5$)$_3$]$^-$ (5). In an argon-filled glovebox, a 20 mL glass reactor was charged with **1** (18.2 mg, 0.03 mmol), B(C_6F_5)$_3$ (15.4 mg, 0.03 mmol), and 2 mL of CD_2Cl_2. The resulting dark red solution was stirred for 30 min at ambient temperature, after which it was filtered. The filtrate was first analyzed by NMR showing the clean formation of **5**, then the solvent of which was removed in vacuo to give 24.9 mg of complex **5** (72%) as a red solid. Anal. Calcd for $C_{52}H_{42}BF_{15}O_4Zr$: C, 55.87; H, 3.79. Found: C, 55.85; H, 3.60.

^{1}H NMR (CD_2Cl_2, 21 °C) for **5**: δ 8.06 (d, J = 8.4 Hz, 1H), 7.94 (d, J = 8.4 Hz, 1H), 7.39−7.22 (m, 6H), 6.29 (d, J = 3.0 Hz, 3H), 5.97 (d, J = 3.0 Hz, 1H), 4.33 (sept, J = 6.4 Hz, 1H, C*H*Me$_2$), 4.14−3.95 (m, 4H, CH_2CH_2), 3.62 (s, br, 1H, C*H*Me$_2$), 1.54 (s, 3H, =C*Me*$_2$), 1.38 (d, J = 6.0 Hz, 3H, CH*Me*$_2$), 1.27 (d, J = 6.0 Hz, 6H, CH*Me*$_2$), 1.21 [s, br, 9H, *Me*'s for =C*Me*$_2$ (3H), CH*Me*$_2$ (3H), and C*Me*$_2$ (3H)], 1.02 (s, br, 3H, C*Me*$_2$). ^{19}F NMR (CD_2Cl_2, 21 °C): δ −132.30 (d, $^3J_{F-F}$ = 19.5 Hz, 6F, *o*-F), −163.09 (t, $^3J_{F-F}$ = 19.5 Hz, 3F, *p*-F), −165.94 (m, 6F, *m*-F). ^{13}C NMR (CD_2Cl_2, 21 °C, only key resonances shown): δ 192.47 [*C*(O^{i}Pr)=O], 150.08 [O*C*(O^{i}Pr)=], 69.02 (O*C*HMe$_2$).

General Polymerization Procedures. Polymerizations were performed in 25 mL flame-dried Schlenk flasks interfaced to the dual-manifold Schlenk line. In a typical procedure, a predetermined amount of Al(C_6F_5)$_3$ was first dissolved in MMA (9.35 mmol) inside a glovebox, and the polymerization was started by rapid addition of this in-situ-prepared alane−MMA solution via a gastight syringe to a 10 mL CH_2Cl_2 solution of **1** under vigorous stirring at the preequilibrated bath temperature. (The amount of MMA was fixed for all polymerizations, and the amounts of Al(C_6F_5)$_3$ and **1** were adjusted according to the ratios specified in the polymerization tables.) After the measured time interval, the polymerization was quenched by the addition of 5 mL of 5% HCl-acidified methanol. The quenched mixture was precipitated into 100 mL of methanol, stirred for 1 h, filtered, washed with methanol, and dried in a vacuum oven at 50 °C overnight to a constant weight.

Polymerization Kinetics. Kinetic experiments were carried out in stirred 25 mL Schlenk flasks at a given temperature using stock solutions of the catalyst. Aliquots (0.2 mL) were taken at appropriate time intervals, treated, and analyzed according to literature procedures.[2b,15]

Polymer Characterizations. Glass transition temperatures (T_g) of the polymers were measured by differential scanning calorimetry (DSC) on a DSC 2920, TA Instruments. Samples were first heated to 180 °C at 20 °C/min, equilibrated at this temperature for 4 min, and cooled to −60 °C at 20 °C/min. After being held at this temperature for 4 min, the samples were then reheated to 180 °C at 10 °C/min. All T_g values were obtained from the second scan, after removing the thermal history. Gel permeation chromatography (GPC) analyses of the polymers were carried out at 40 °C and a flow rate of 1.0 mL/min, with $CHCl_3$ as the eluent, on a Waters University 1500 GPC instrument equipped with four 5 μm PL gel columns (Polymer Laboratories) and calibrated using 10 PMMA standards. Chromatograms were processed with Waters Empower software (version 2002). NMR spectra for the polymers were recorded in $CDCl_3$ and analyzed according to literature procedures.[16]

X-ray Crystallographic Analysis of 2. Single crystals of complex **2** grown from toluene were quickly covered with a layer of Paratone-N oil (Exxon, dried and degassed at 120 °C/10^{-6} Torr for 24 h), after the mother liquors were decanted, and then mounted on a thin glass fiber and transferred into the cold nitrogen stream of a Bruker SMART CCD diffractometer. The structure was solved by direct methods and refined using the Bruker SHELXTL program library by full-matrix least-squares on F^2 for all reflections.[17] All non-hydrogen atoms were refined with anisotropic displacement parameters, whereas hydrogen atoms were included in the structure factor calculations at idealized positions. There is a toluene molecule found in the lattice. Selected crystallographic data for **2**·C_7H_8: $C_{76}H_{48}Al_2F_{30}O_5Zr$, triclinic, space group $P\bar{1}$, a = 10.3530(6) Å, b = 16.3085(10) Å, c = 21.7857(13) Å, α = 83.8880(10)°, β = 80.7960(10)°, γ = 76.1090(10)°, V = 3515.9(4) Å^3, Z = 2, D_{calcd} = 1.658 mg/m^3, $R1$ = 0.0531 [$I > 2\sigma(I)$], $wR2$ = 0.1134.

Results and Discussion

Polymerization Characteristics. Table 1 summarizes representative results of MMA polymerization by the **1**/2Al(C_6F_5)$_3$ system in CH_2Cl_2 in a [MMA]$_0$/[**1**]$_0$ ratio ranging from 600 to 1500. It must be noted here that the catalyst Al(C_6F_5)$_3$ and the solvent CH_2Cl_2 are incompatible if directly mixed as CH_2Cl_2 decomposes Al(C_6F_5)$_3$ via chloride abstraction to form (C_6F_5)$_2$-AlCl that has been structurally characterized as a dimer in the solid state.[18] Conversely, CH_2Cl_2 presents no problems for reactions using the alane in the form of a base adduct such as Al(C_6F_5)$_3$·THF and Al(C_6F_5)$_3$·MMA. Additionally, direct contact of Al(C_6F_5)$_3$ with **1** leads to rapid decomposition as well. Thus, in the present polymerization system, it is critical that Al(C_6F_5)$_3$ be first mixed (dissolved) in large excess MMA (the amount of which depends on the [MMA]$_0$/[**1**]$_0$ ratio employed) followed by addition to a CH_2Cl_2 solution of **1** to start the polymerization. (All elementary reactions involving these reagents when mixed in different sequences will be thoroughly discussed later.) As can be seen from Table 1, the polymerization at 22 °C with a relatively high concentration of [**1**] = 1.50 mM, which corresponds to a [MMA]$_0$/[**1**]$_0$ ratio of 600, is rapid and produces essentially *st*-P(MMA) with nearly constant *st* ([*rr*] = 68−71%) and *ht* (heterotactic, [*mr*] = 22−24%) indices vs monomer conversion (runs 1−10, Table 1). Number-average molecular weights (M_n) of the resulting polymers at various

Table 1. Selected MMA Polymerization Results by the 1/2Al(C_6F_5)$_3$ System[a]

run no.	[**1**] (mM)	$[MMA]_0/[\mathbf{1}]_0$	temp (°C)	time (min)	conv (%)	$10^4 M_n$[b] (g/mol)	PDI[b] (M_w/M_n)	[*mm*][c] (%)	[*mr*][c] (%)	[*rr*][c] (%)
1	1.56	600	22	1	38	2.08	1.54	6.6	22.1	71.3
2				2	45	2.24	1.50	7.0	23.1	69.9
3				3	52	2.15	1.54	7.2	22.7	70.1
4				4	56	2.37	1.47	7.2	22.6	70.2
5				5	60	2.37	1.48	7.8	23.7	68.5
6				6	67	2.34	1.51	6.9	24.0	69.1
7				7	72	2.50	1.50	8.3	23.7	68.0
8				8	76	2.56	1.49	8.9	22.6	68.5
9				9	82	2.82	1.47	8.7	23.4	67.9
10				10	88	2.92	1.43	8.6	23.7	67.7
11	1.17	800	22	1	7	0.66	1.32	32.5	19.0	48.5
12				5	16	0.95	1.38	36.7	18.2	45.1
13				10	24	1.37	1.36	40.7	17.1	42.2
14				15	32	1.77	1.34	42.4	16.5	41.1
15				20	40	2.26	1.30	42.7	16.7	40.6
16				25	48	2.63	1.27	44.3	16.0	39.7
17				30	55	3.04	1.25	44.7	15.9	39.4
18				35	62	3.32	1.24	44.5	16.2	39.3
19				40	70	3.46	1.23	44.2	16.4	39.4
20				46	75	4.05	1.22	45.0	16.1	38.9
21				50	81	4.04	1.22	44.2	16.3	39.5
22				60	91	4.64	1.20	41.9	16.8	41.3
23				70	100	5.05	1.20	40.0	17.4	42.6
24	1.17	800	0	2	17	0.83	1.61	18.7	19.4	61.9
25				10	25	1.48	1.38	21.7	17.9	60.4
26				20	38	2.21	1.32	21.2	18.0	60.8
27				30	49	2.91	1.27	22.9	18.5	58.6
28				40	57	3.46	1.24	21.5	18.1	60.4
29				55	71	4.18	1.24	21.3	18.0	60.7
30				70	86	4.93	1.24	22.0	18.8	59.2
31				104	95	5.80	1.24	20.7	18.1	61.2
32	0.935	1000	22	5	12	0.90	1.31	38.5	17.6	43.9
33				7	14	1.09	1.33	41.4	18.2	40.4
34				10	23	1.40	1.33	46.2	16.8	37.0
35				15	29	1.85	1.32	45.7	17.1	37.3
36				20	34	2.12	1.35	47.8	16.3	35.9
37				30	46	2.89	1.30	47.5	15.8	36.7
38				45	62	3.91	1.27	50.2	15.5	34.3
39				75	84	5.01	1.34	54.1	14.4	31.5
40				120	94	5.55	1.23	56.0	13.8	30.2
41				180	98	6.10	1.34	60.9	12.6	26.5
42	0.935	1000	0	4	15	0.60	1.31	39.0	18.8	42.2
43				10	21	0.99	1.25	40.6	15.8	43.6
44				20	31	1.52	1.24	42.0	15.7	42.3
45				30	42	2.01	1.24	43.3	15.0	41.7
46				45	45	2.78	1.20	41.0	15.6	43.4
47				60	52	3.36	1.19	43.7	14.9	41.4
48				90	66	4.22	1.18	47.2	14.2	38.6
49				120	77	5.15	1.18	48.8	13.8	37.4
50				181	88	5.73	1.19	52.5	13.0	34.5
51				240	92	5.97	1.20	54.4	12.5	33.1
52	0.78	1200	22	2	12	0.58	1.32	52.9	18.2	28.9
53				6	14	1.40	1.41	64.8	13.7	21.5
54				10	20	2.10	1.43	69.3	12.3	18.4
55				15	24	2.54	1.52	70.1	12.1	17.8
56				20	28	3.21	1.47	71.3	12.2	16.5
57				30	43	4.19	1.43	71.0	12.1	16.9
58				45	58	5.50	1.38	73.9	10.9	15.2
59				60	67	5.98	1.34	73.4	10.8	15.8
60				90	82	6.90	1.34	71.6	11.7	16.7
61				120	89	6.95	1.38	72.5	11.3	16.2
62				150	93	7.87	1.37	74.7	10.6	14.7
63	0.62	1500	22	5	9	2.16	1.17	77.2	12.7	10.1
64				11	18	3.72	1.28	80.1	11.3	8.6
65				20	22	5.24	1.38	84.1	9.1	6.8
66				30	31	6.65	1.41	81.5	10.6	7.9
67				45	43	8.06	1.42	80.3	11.0	8.7
68				60	53	9.46	1.44	81.7	10.4	7.9
69				90	64	9.88	1.54	80.9	10.7	8.4
70				120	72	9.65	1.61	81.2	10.6	8.2

[a] Carried out in Schlenk flasks on a Schlenk line using an external temperature-control bath, 10 mL of CH_2Cl_2. [b] Number-average molecular weight (M_n) and polydispersity index (PDI) determined by GPC relative to PMMA standards in $CHCl_3$. [c] Tacticity (methyl triad distribution) determined by ^1H NMR spectroscopy.

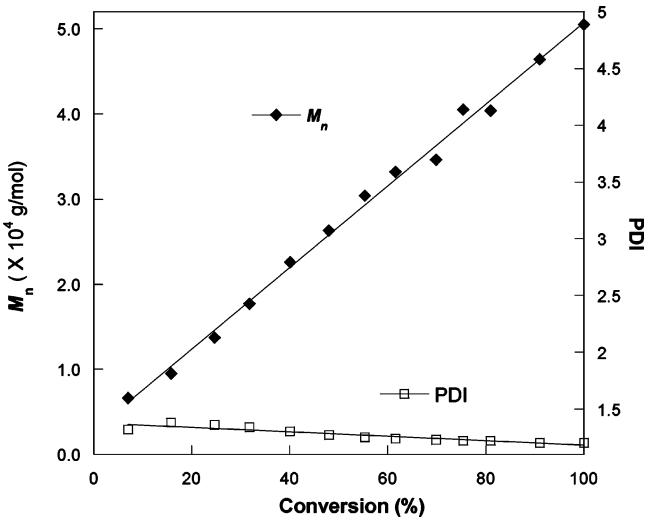

Figure 1. Plot of M_n and PDI of P(MMA) by the **1**/2Al(C_6F_5)$_3$ system {[MAA]$_0$/[**1**]$_0$ = 800; 22 °C} vs monomer conversion.

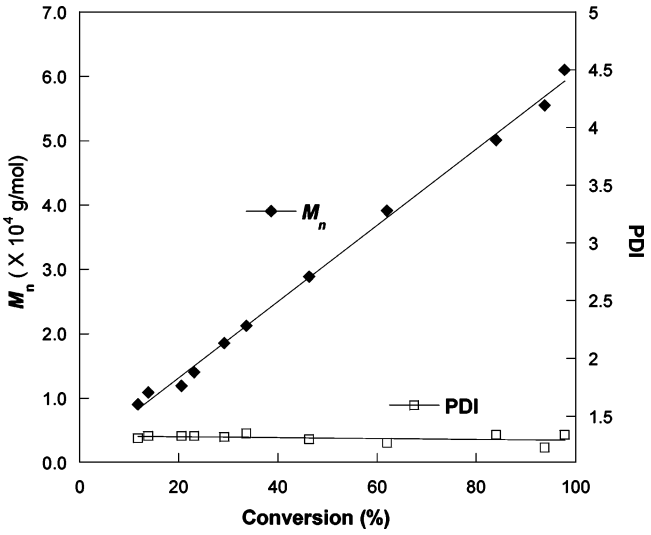

Figure 2. Plot of M_n and PDI of P(MMA) by the **1**/2Al(C_6F_5)$_3$ system {[MAA]$_0$/[**1**]$_0$ = 1000; 22 °C} vs monomer conversion.

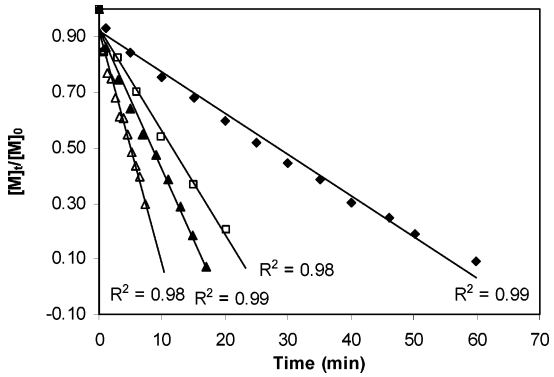

Figure 3. Selected zero-order plots of $[M]_t/[M]_0$ vs time for the polymerization of MMA by **1**/*x*Al(C_6F_5)$_3$ in CH_2Cl_2 at 22 °C. Conditions: [MMA]$_0$/[Al]$_0$/[Zr]$_0$ = 800/2/1 (◆), 800/3/1 (□), 800/4/1 (▲), and 800/5/1 (△).

conversions indicate that approximately two polymer chains were produced per Zr center. For example, at 67% conversion, the measured M_n was 2.34 × 10^4 compared to the calculated M_n of 2.01 × 10^4 based on 2[MMA]$_0$/[I]$_0$ = 600, giving an initiator efficiency [*I** = M_n(calcd)/M_n(exptl), where M_n(calcd) = MW(MMA) × [MMA]$_0$/[I]$_0$ × conversion %] of 86%. Likewise, the *I** was calculated to be 87% at a conversion of 82%; these *I** values are typical of those MMA polymerizations by the metallocene system.[2b] All polymers produced exhibit unimodal molecular weight distributions (MWD) with polydispersity indices (PDI = M_w/M_n) ranging from 1.43 to 1.54.

The polymerization in a [MMA]$_0$/[**1**]$_0$ ratio of 800 at 22 °C is considerably slower and achieves quantitative monomer conversion in 70 min (runs 11−23, Table 1), but the M_n data of the resulting polymers are still consistent with the production of two polymer chains per Zr center. However, the polymerization at this ratio is more controlled in terms of an observed linear increase of the polymer M_n with monomer conversion, which is coupled with relatively small and nearly constant PDI values (Figure 1). More significantly, the polymers produced exhibit *it-b-st sb*-microstructures,[8] with enriched in both *st* ([*rr*] = 40−45%) and *it* ([*mm*] = 43−39%) contents as well as reduced *ht* contents ([*mr*] = 16−17%). The polymers produced are unimodal with relatively narrow MWDs as measured by GPC in either THF (stereocomplex solvent) or $CHCl_3$ (no complex solvent), exhibit single T_g values ranging from 93 to 99 °C, and show practically no change in stereomicrostructures (triad distributions) with quantitative recovery yields after they have been extracted by boiling absolute ethanol for >12 h [*it*-P(MMA) of medium molecular weight (M_n < 5 × 10^4) is soluble in hot ethanol[2n]]; the combined above evidence supports the conclusion that these polymers produced by the **1**/2Al(C_6F_5)$_3$ system under these conditions are *it-b-st* multiblock P(MMA), implying that the polymerization occurs in a diastereospecific fashion. Polymerizations at 0 °C (runs 24−31, Table 1) behave similarly, except that the resulting polymers have ∼20% more *st* contents than those produced at 22 °C.

A further decrease in the concentration of **1** to reach a [MMA]$_0$/[**1**]$_0$ ratio of 1000 further slows down the polymerization at 22 °C (runs 32−41, Table 1); however, the M_n data of the resulting polymers are still consistent with the production of two polymer chains per Zr center. Under this condition, there is a gradual increase in *it* content from [*mm*] = 39% to 61% as monomer conversion increases from 12% to 98%, and conversely the *st* content decreases from [*rr*] = 44% to 27%; in the same conversion window, the *ht* content remained relatively low ([*mr*] = 18−13%). The polymerization also shows a linear increase of the polymer M_n vs monomer conversion with relatively small, nearly constant PDI values (Figure 2). Using the same analytical procedures employed for the polymers produced at the 800:1 ratio, all polymers produced at the 1000:1 ratio are confirmed to be *it-b-st* multiblock P(MMA), but they have considerably longer *it* sequences. Polymerizations at 0 °C (runs 42−51, Table 1) produce polymers with similar characteristics. Polymerizations under a further reduced catalyst concentration in MMA]$_0$/[**1**]$_0$ ratio of 1200 (runs 52−62) give polymers with increasingly more *it* contents than *st* contents in the *it-b-st sb*-P(MMA) product, with [*mm*] reaching ∼70%. Lastly, when the catalyst concentration is further reduced to such that the MMA]$_0$/[**1**]$_0$ ratio = 1500, the resulting polymers are essentially *it*-P(MMA) with nearly constant *it* content of [*mm*] ∼80%.

Polymerization Kinetics. MMA polymerizations by the **1**/2Al(C_6F_5)$_3$ system with relatively high catalyst concentrations of [**1**] ≥ 1.17 mM (i.e., [MMA]$_0$/[**1**]$_0$ ≤ 800) at 22 °C follow zero-order kinetics in [MMA] (Figure 3); this kinetic behavior holds true for the polymerizations at 0 °C despite the expected lower rates. Varying the equivalency of Al(C_6F_5)$_3$ employed did not alter this kinetic order (Figure 3), and analyses of the resulting polymer by the **1**/*x*Al(C_6F_5)$_3$ system (*x* = 2−5) showed similar polymer M_n and PDI values at nearly the same monomer

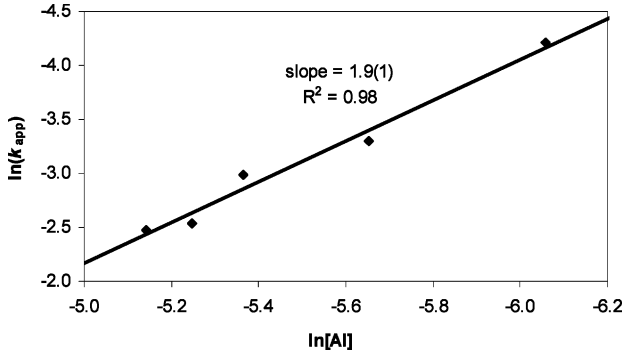

Figure 4. Plot of $\ln(k_{app})$ vs ln[Al] for the MMA polymerization by **1**/*x*Al$(C_6F_5)_3$ at 22 °C.

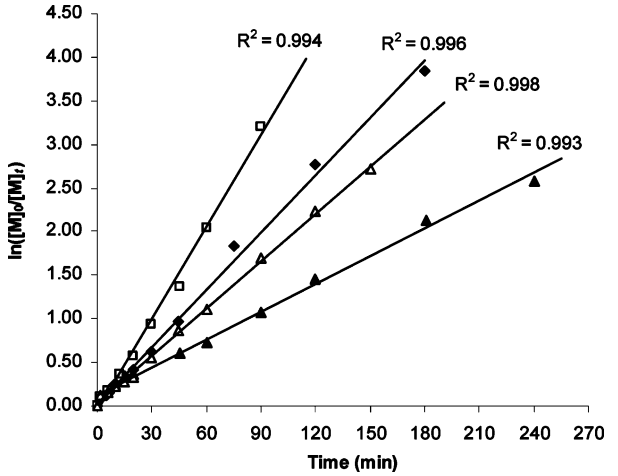

Figure 5. Selected first-order plots of $\ln([M]_0/[M]_t)$ vs time for the polymerization of MMA by **1**/*x*Al$(C_6F_5)_3$ in CH_2Cl_2. Conditions: $[MMA]_0/[Al]_0/[Zr]_0$ = 1000/3/1 at 22 °C (□), 1000/2/1 at 22 °C (◆), 1200/2/1 at 22 °C (△), and 1000/2/1 at 0 °C (▲).

conversions although the *st* content of the resulting P(MMA) gradually increased from ∼40% to ∼60% when *x* was varied from 2 to 5. A double-logarithm plot (Figure 4) of the apparent rate constants (k_{app}), which were obtained from the slopes of the best-fit lines to the plots of $[MMA]_t/[MMA]_0$ vs time, as a function of [Al$(C_6F_5)_3$], was fit to a straight line of slope = 1.9(1). Hence, the kinetic order with respect to [Al$(C_6F_5)_3$], given by the slope of 1.9(1), reveals that propagation is approximately second order in [Al$(C_6F_5)_3$] under the concentration regime defined above.

On the other hand, MMA polymerizations by the **1**/2Al$(C_6F_5)_3$ system with relatively low zirconocene concentrations of [**1**] ≤ 0.935 mM (i.e., $[MMA]_0/[\mathbf{1}]_0 \geq 1000$) at 22 °C follow strictly first-order kinetics in [MMA] (Figure 5). As can be seen from this figure, the first-order kinetics within this concentration regime is invariant of both the **1**/Al$(C_6F_5)_3$ ratio (with 2 equiv of the alane or greater) and reaction temperature.

Elementary Reactions. There are four possible elementary reactions to consider in the current polymerization system containing the monomer MMA as well as catalysts zirconocene bis(ester enolate) **1** and Lewis acid Al$(C_6F_5)_3$. First, there was no reaction between MMA and **1** under the polymerization conditions employed (in CH_2Cl_2 at ambient temperature up to several hours). Second, mixing of MMA and Al$(C_6F_5)_3$ spontaneously forms the adduct Al$(C_6F_5)_3$·MMA. Third, direct contact of **1** with Al$(C_6F_5)_3$ in toluene led to the formation of a mixture of unidentified species. Decomposition of the analogous mono-ester enolate complex, *rac*-(EBI)ZrMe[OC(O^{i}Pr)═CMe$_2$], by Al$(C_6F_5)_3$ was reported to occur via the alane-assisted 1,5-H sigmatropic shift of β-H of the isopropoxy group to the ═*C*Me$_2$ carbon followed by elimination of propylene and formation of the carboxylate bridged ion pair.[2f] In the current polymerization system, however, at no time does the free Al$(C_6F_5)_3$ exist because it is always in the form of an adduct with either MMA or the ester group of the polymer chain. Thus, the fourth elementary reaction consider is the reaction of **1** with the adduct Al$(C_6F_5)_3$·MMA, which is precisely related to the current polymerization system and identical to our practice (i.e., we premix the alane with excess MMA to form the adduct before addition to a CH_2Cl_2 solution of **1** to start the polymerization; vide supra). Significantly, unlike the complex decomposition reactions observed upon mixing of **1** and Al$(C_6F_5)_3$, the reaction of **1** with Al$(C_6F_5)_3$·MMA yielded no such complex decomposition products, but clean and characterizable species. Thus, the reaction of **1** with 2 equiv of Al$(C_6F_5)_3$·MMA in CH_2Cl_2 for 24 h (to ensure a complete conversion of **1** and other related species shown in Scheme 1 to **2**) at ambient temperature afforded ion pair **2** as an orange-red crystalline solid in 76% isolated yield. The cation portion of **2** is identical to the living, highly isospecific, cyclic ester enolate zirconocenium cation that is paired with the methyl borate anion, *rac*-(EBI)Zr[OC(OMe)═C(Me)CH$_2$C(Me$_2$)C(O^{i}Pr)═O]$^+$[MeB$(C_6F_5)_3]^-$, which was derived from the single MMA addition to *rac*-(EBI)Zr$^+$(THF)-[OC(O^{i}Pr)═CMe$_2$][MeB$(C_6F_5)_3]^-$ and previously isolated as well as spectroscopically/analytically (but not structurally) characterized;[2b] the cation is also an isoelectronic structure of the neutral samarium complex $(C_5Me_5)_2$Sm$(MMA)_2$H, which was isolated from the reaction of the samarium hydride precursor with 2 equiv of MMA and crystallographically characterized.[19]

X-ray diffraction analysis of single crystals of **2** confirmed the molecular structure inferred from spectroscopic and analytical data, featuring unassociated cation and anion pairs (Figure 6). The structural motif of the cation is indeed that of the proposed chiral *ansa*-zirconocenium center incorporating the *rac*-(EBI) ligand and eight-membered-ring cyclic ester enolate moiety,[2b] whereas the anion is a methoxy-bridged dialuminate in which the bridging oxygen adopts a trigonal-planar geometry with a sum of the angles around the oxygen of 359.9°. The covalent Zr−enolate oxygen bond [Zr−O(2) = 1.987(3) Å] is noticeably shorter than the dative Zr−carbonyl oxygen bond [Zr−O(1) = 2.117(3) Å] by 0.13 Å, whereas the enolate carbon−oxygen single bond [C(22)−O(2) = 1.361(5) Å] is longer than the C═O double bond [C(29)−O(1) = 1.247(4) Å] by 0.11 Å. The C(22)═C(24) double bond is characterized by a bond distance of 1.322(6) Å and a sum of the angles around C(22) of 360.0° for a trigonal-planar geometry. Interestingly, the O(1)−Zr−O(2) angle of 97.4(1)° in **2** is identical to that observed in the precursor bis(ester enolate) **1**, despite its formation of the eight-membered-ring cyclic ester enolate moiety that adopts an unusual conformation in which both the enolate oxygen atom O(2) and the methylene carbon atom C(25) are located above the plane defined approximately by the remaining ring atoms. On the other hand, unlike the partial double-bond character for the Zr−O bond in **1** where the oxygen is partly sp-hybridized due to a $p_\pi-d_\pi$ interaction between zirconium and enolate oxygen,[2f] the Zr−enolate oxygen bond in **2** is purely a single bond, as evidenced by its bond length and a small Zr−O(2)−C(22) vector angle of 125.2(2)°, presumably as a consequence of the eight-membered-ring conformation. This unique ring conformation places the C(27) atom, equivalent of the growing polymer chain (which would make the C(26) the chiral penultimate chain end), in the coordination sphere voids of the *rac*-(EBI) ligand structure, facing away from the C$_6$-

Scheme 1

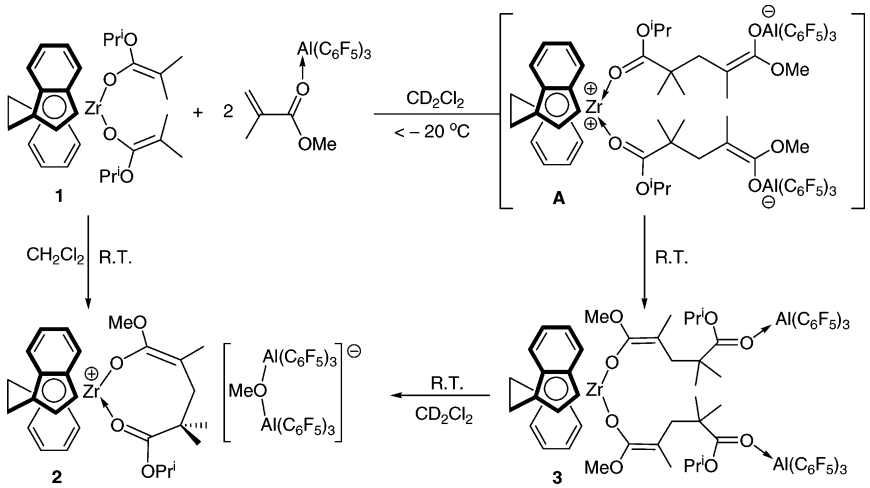

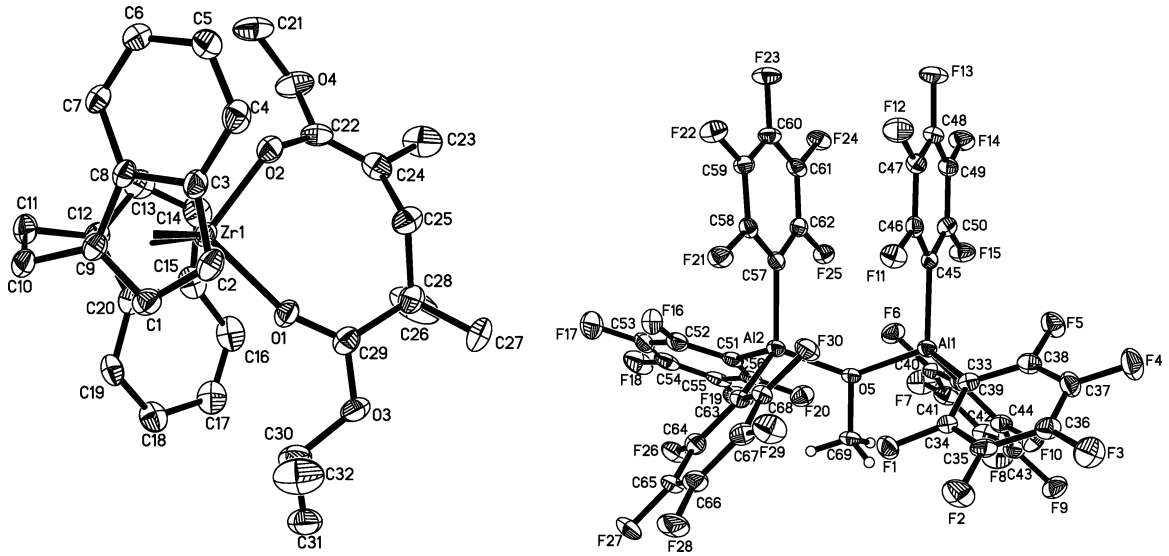

Figure 6. Molecular structure of **2**. Selected bond lengths (Å): Zr−O(1) = 2.117(3), Zr−O(2) = 1.987(3), C(29)−O(1) = 1.247(4), C(29)−O(3) = 1.303(4), C(22)−O(2) = 1.361(5), C(22)−O(4) = 1.373(5), C(22)−C(24) = 1.322(6), Al(1)−O(5) = 1.846(3), Al(2)−O(5) = 1.831(3). Selected bond angles (deg): Zr−O(1)−C(29) = 159.9(3), Zr−O(2)−C(22) = 125.2(2), O(1)−Zr−O(2) = 97.4(1), Al(1)−O(5)−Al(2) = 138.6(2).

rings of the bridged indenyl ligands and also avoiding the steric congestion with the vinyl methyl C(23) atom with approximately a trans arrangement between these two groups. This interplay between the chirality of the C_2 ligand and the growing penultimate chain end as well as the vinyl methyl group presumably determines how the incoming MMA approaches and ring opens this active resting cyclic enolate intermediate—the rate-limiting step of the polymerization[2b]—and thus the isospecificity of this cation.

Monitoring the reaction of **1** + 2[Al(C_6F_5)$_3$·MMA] in CD_2Cl_2 by VT NMR revealed, upon mixing of these two reagents at −78 °C, spontaneous formation of a deep red solution, characteristic of zirconocenium dication formation;[20a,b] spectroscopic data are also consistent with formation of intermediate **A**, shown in Scheme 1, comprising the zirconocenium dication[20a,b] paired with enolaluminate anions.[15] This dicationic intermediate is thermally unstable; on warming to about −20 °C, it begins to undergo ester−enolate isomerization to form yellowish neutral zirconocene bis(ester enolate) complex **3** in which both terminal ester carbonyl oxygen atoms are coordinated to Al(C_6F_5)$_3$. Further standing of the resulting yellow solution of **3** at ambient temperature induced a graduate transformation of neutral complex **3** to cationic complex **2** as outlined in Scheme 1. These two complexes can be readily distinguished by ^{1}H and ^{19}F NMR; while there are four sets (doublets) of signals for the four C_5-ring protons in ^{1}H NMR of complex **2** (C_1 symmetry), there are only two sets of signals for the four C_5-ring protons in complex **3** as a consequence of C_2 symmetry. The enolate *Me*O group exhibits similar chemical shifts in both complexes (δ 3.14 ppm in **2** vs 2.99 ppm in **3**), but the second *Me*O group in **2** is linked to two Al centers in the anion (δ 4.05 ppm). The coordinated isopropyl ester group [−C(O^{i}Pr)═O] also gives rise to sharply different chemical shifts, depending on whether the carbonyl oxygen is coordinated to Zr in **2** or Al in **3**; specifically, the ^{1}H NMR signal for −OC*H*Me$_2$ (sept, 4.34 ppm) in **2** is considerably downfield shifted to 5.19 ppm (sept) for −OC*H*Me$_2$ in **3**. Lastly, the ^{19}F NMR chemical shift difference further confirms their structural assignments; a further upfield shift for the *para*- and *meta*-fluorines and a smaller chemical shift difference between the *para*- and *meta*-fluorines in ion pair **2**, as compared to those observed in neutral complex **3**, are consistent with the anionic nature of the aluminate moiety[20] in **2** vs the datively coordinated neutral alane moiety in complex **3** that shows a nearly identical ^{19}F NMR spectrum to Al(C_6F_5)$_3$·MMA. It is noteworthy that, owing to this transformation in polar solvents such as CH_2Cl_2 (the conversions of **3** to **2** in CD_2Cl_2 at 23 °C were 8% and 36% for 20 min and 2 h, respectively), isolation of the yellow neutral complex **3** in pure

Scheme 2

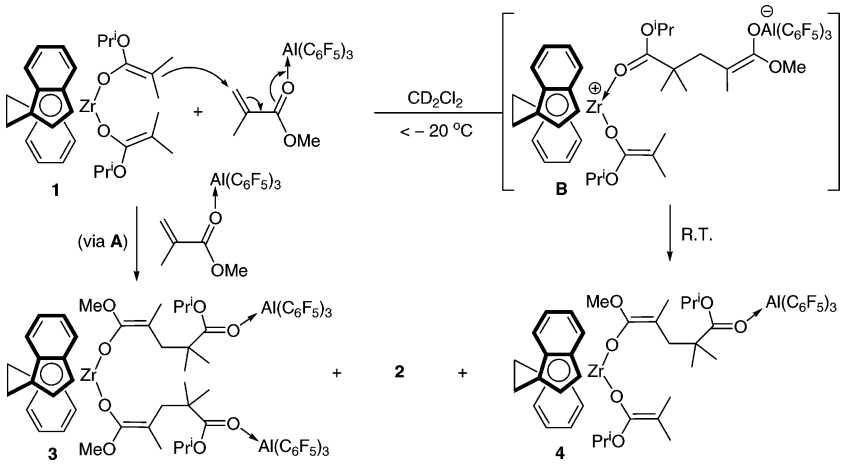

Scheme 3

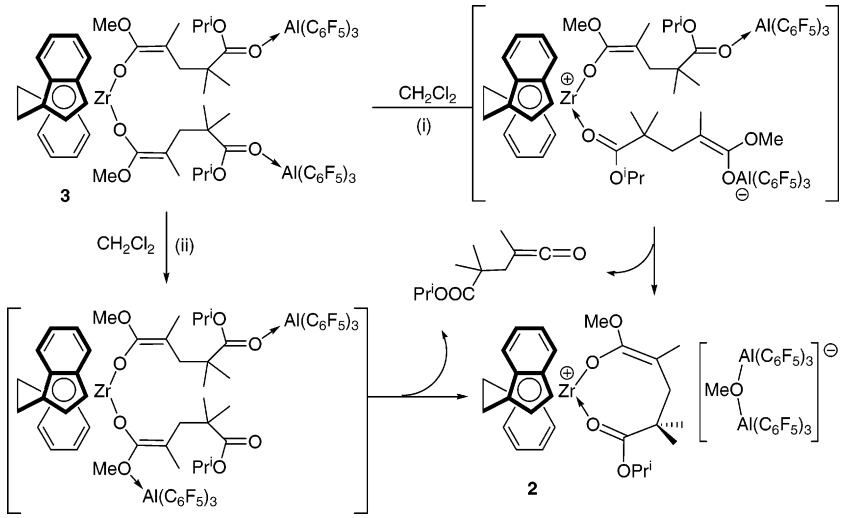

state was achieved only from the **1** + 2[$Al(C_6F_5)_3$·MMA] reaction in hexanes at ambient temperature for 30 min, the conditions of which suppressed the formation of **2**.

We also investigated the reaction of **1** with 1 equiv of Al-($C_6F_5)_3$·MMA in CH_2Cl_2, which was found to occur analogously to the 1:2 ratio reaction. Under this ratio, however, both dicationic **A** and monocationic **B** intermediates (plus the remaining unreacted **1**) were generated at low temperatures, which, upon warming to ambient temperature, led to formation of a mixture containing neutral complexes **3** and **4** as well as the cationic complex **2** (Scheme 2), depending on how long the solution mixture was kept at this temperature. Complexes **3** and **4** can be readily distinguished by ^{1}H NMR (see Experimental Section), most notably, the splitting pattern of the *rac*-(EBI) moiety due to differences in symmetry (C_2 for **3** vs C_1 for **4**) and the type of the O^{i}Pr group present due to differences in linkage (identical two ester O^{i}Pr groups in **3** vs different one ester and one enolate O^{i}Pr groups in for **4**); however, isolation of complex **4** in pure state by separation of these two complexes in a preparative scale proved unfeasible. When the reaction of **1** with 1.3 equiv of $Al(C_6F_5)_3$·MMA (to ensure a complete consumption of **1**) was carried out in hexanes (to suppress the formation of **2**), the formation of **4** was accompanied by ~40% of **3**; attempts to separate them by recrystallization were unsuccessful. Nevertheless, the observation for the formation of intermediate **B** and complex **4** adds additional important pieces to the overall polymerization mechanism described later.

Two possible pathways for converting neutral complex **3** to cationic complex **2** are proposed in Scheme 3. Pathway i proceeds via enolate−ester isomerization, formally abstraction of the enolate moiety by the alane, to the cationic ester enolate intermediate analogous to **B** that undergoes methoxide abstraction by the alane followed by elimination of a ketene and ring closure to form complex **2**. On the hand, pathway ii proceeds via a nonionic intermediate derived from migration of the alane from the carbonyl oxygen to the enolate methoxy oxygen to effect methoxide abstraction there followed by the ketene elimination and ring closure to give **2**. The observed significant rate acceleration in noncoordinating polar solvent CH_2Cl_2 over toluene and no conversion in nonpolar hexane solvent suggest that pathway i is presumably operative.

Temperature and Lewis Acid Effects. When the polymerization temperature decreased from 22 to −40 °C at the constant catalyst concentration ([**1**] = 1.17 mM) and ratio ([MMA]$_0$/[Al]$_0$/[**1**]$_0$ = 800/2/1), the time required for achieving quantitative monomer conversion increased gradually from 70 to 120 min, and the resulting polymer *st* content and molecular weight increased gradually to afford essentially *st*-P(MMA) at −20 ([*rr*] = 81%) and −40 °C ([*rr*] = 83%), as shown in Table 2. These results imply that, as the reaction temperature decreases, the bimolecular propagation process brought about by the Al catalyst that produces the *st*-blocks becomes increasingly more competitive than the monometallic propagation process operated by the Zr catalyst that yields the *it*-blocks.

Table 2. Comparisons of the P(MMA) at Quantitative Conversions at Varied Temperatures[a]

run no.	temp (°C)	10^4M_n (g/mol)	PDI (M_w/M_n)	[*mm*] (%)	[*mr*] (%)	[*rr*] (%)
1	22	5.05	1.20	40.0	17.4	42.6
2	0	5.80	1.26	21.4	18.8	59.8
3	−20	6.37	1.54	2.7	16.2	81.1
4	−40	7.05	1.87	3.1	13.8	83.1

[a] See Table 1 footnotes for explanations of the abbreviations listed in this table; conditions: [**1**] = 1.17 mM, $[MMA]_0/[Al]_0/[\mathbf{1}]_0$ = 800/2/1.

Table 3. Selected MMA Polymerization Results by the 1/2MeAl(BHT)$_2$ System [a]

run no.	time (h)	conv (%)	10^4M_n (g/mol)	PDI (M_w/M_n)	[*mm*] (%)	[*mr*] (%)	[*rr*] (%)
1	0.5	10	2.42	1.84	79.7	14.6	5.7
2	1	13	4.07	2.39	88.1	7.9	4.0
3	2	22	7.20	2.39	88.4	7.9	3.7
4	3	30	8.68	2.29	86.5	8.8	4.7
5	4	37	9.37	2.14	84.8	9.7	5.5
6	5	43	15.7	1.54	85.8	9.5	4.7
7	6	50	9.62; 4960[b]	2.00; 1.27[b]	85.6	9.6	4.8
8	8	61	9.70; 2725[b]	1.94; 1.31[b]	86.6	8.6	4.8
9	10	69	10.9; 1749[b]	1.92; 1.24[b]	84.4	10.1	5.5
10	12	78	10.4; 1068[b]	1.92; 1.28[b]	82.7	10.5	6.8
11	15	85	9.56; 507[b]	2.09; 1.24[b]	85.1	9.6	5.3

[a] See Table 1 footnotes for explanations of the abbreviations listed in this table; conditions: [**1**] = 0.935 mM, $[MMA]_0/[\mathbf{1}]_0$ = 1000, 22 °C. [b] A bimodal distribution with a small high-molecular-weight tail.

A seemingly analogous system comprising **1** and B(C_6F_5)$_3$ (1 or 2 equiv) gave no formation of the *sb*-polymer but simply highly *it*-P(MMA). To seek for an answer to this observation, we examined the 1:1 ratio reaction of **1** and B(C_6F_5)$_3$ and found that it forms cationic zirconocene ester enolate−α-ester borate ion pair **5** (Scheme 4) as a result of apparent electrophilic addition of the borane to the nucleophilic ester enolate α-carbon, reminiscent of the reaction of B(C_6F_5)$_3$ with the sterically unprotected bis(2-propenolato)zirconocene reported by Erker et al.[21] The reaction with 2 equiv of B(C_6F_5)$_3$ affords the same product with no indication of the possible bis-adduct formation. The MMA polymerization by the isolated species **5** indeed affords P(MMA) with high isotacticity of [*mm*] = 96% by a site-control mechanism (2[*rr*]/[*mr*] = 1.0) and low polydispersity of PDI = 1.05, showing the similar polymerization behavior to the THF-coordinated cationic *ansa*-zirconocenium ester enolate,[2b] except for somewhat lower activity of **5**. Polymerizations by in-situ mixing of MMA with 1 or 2 equiv of B(C_6F_5)$_3$ followed by addition of complex **1** (i.e., activated monomer approach), or by in-situ mixing of complex **1** with B(C_6F_5)$_3$ followed by addition of MMA (i.e., activated complex approach), gave similarly highly *it*-P(MMA). Overall, the Lewis acid in the **1**/B(C_6F_5)$_3$ system functions only as a cation-forming agent, and neither the resulting anion nor the neutral borane participates in the polymer chain formation steps as do Al(C_6F_5)$_3$ and its derived anions in the **1**/Al(C_6F_5)$_3$ system.

Replacing Al(C_6F_5)$_3$ in the highly effective **1**/2Al(C_6F_5)$_3$ system with common trialkylaluminum reagents such as $AlMe_3$ (2 and 50 equiv) resulted in a completely inactive system for MMA polymerization, while substituting Al(C_6F_5)$_3$ with MeAl(BHT)$_2$ yielded an active system but with substantially lower activity. Additionally, the **1**/2MeAl(BHT)$_2$ system produce simply *it*-P(MMA) with [*mm*] ranging from 80% to 87% and the triads conforming to a site-control mechanism, suggesting that only the isospecific zirconocenium site is operative in this polymerization. Furthermore, the polymers produced at monomer conversions ≥50% after 6 h showed bimodal molecular weight distributions with small high-molecular-weight tails

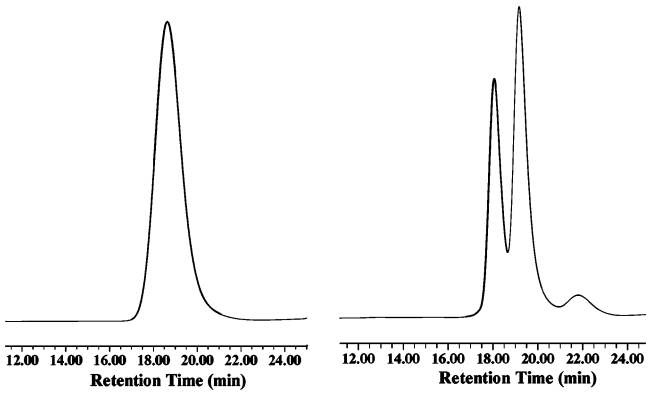

Figure 7. Representative GPC traces of P(MMA) by the **1**/2Al(C_6F_5)$_3$ system (left; PDI = 1.20 in this example) and by the **1**/2Cp$_2$Zr[OC(O^{i}Pr)=CMe$_2$)]$^+$MeB(C_6F_5)$_3^-$ system (right, multimodal MWD) both in a $[MAA]_0/[\mathbf{1}]_0$ = 800 at 22 °C in CH_2Cl_2.

Scheme 4

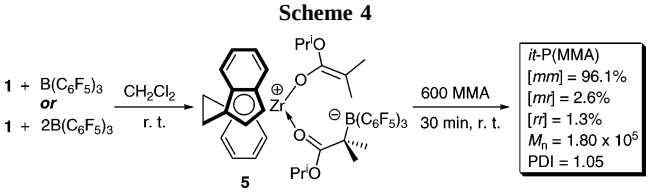

(Table 3). Increasing the amount of MeAl(BHT)$_2$ to 50 equiv with respect to **1** only moderately enhanced the polymerization activity; for example, with a reaction time of 2 h, the conversion reached 38%, which compared to a conversion of 22% with 2 equiv of MeAl((BHT)$_2$, although the resulting polymer exhibits a higher isotacticity ([*mm*] = 91.7%, [*mr*] = 5.5%, [*rr*] = 2.8) again conforming to a site-control mechanism. Lastly, methylaluminoxane (MAO) behaves similarly to MeAl((BHT)$_2$.

MMA polymerizations by **1** in combination with metallocenium-based Lewis acids, rather than Al(C_6F_5)$_3$, were also investigated. Thus, the polymerization of 800 equiv of MMA for 2 h by **1** + 2Cp$_2$Zr[OC(O^{i}Pr)=CMe$_2$)]$^+$MeB(C_6F_5)$_3^-$ (generated by in-situ mixing of Cp$_2$ZrMe[OC(O^{i}Pr)=CMe$_2$)] with B(C_6F_5)$_3$) gave P(MMA) in 92% yield with *sb*-like triad distributions: [*mm*] = 45.0%, [*mr*] = 19.4%, and [*rr*] = 35.6; however, the polymer obtained is not unimodal but exhibits a trimodal MWD (Figure 7), presumably due to a mixture of polymer products derived from the separate isospecific and syndiospecific sites as well as the site-exchange process. The polymerization results using the **1**/2Cp$_2$ZrMe$^+$MeB(C_6F_5)$_3^-$ system were nearly identical, and this polymerization behavior was not significantly affected by the mixing sequence of the reagents. These results argue that interconversion between diastereospecific sites is ineffective (none or much slower than the rate of chain formation).

These above results clearly demonstrate that, among the Lewis acids investigated in this study, only Al(C_6F_5)$_3$ is capable of effecting simultaneous *it*- and *st*-polymer chain formations at the cationic zirconocenium and anionic aluminate sites, respectively, rendering the rate of interconversion between two sites to be faster than the rate of chain formation and thus producing *it-b-st* multiblock P(MMA) with unimodal MWDs.

Polymerization Mechanism. On the basis of the above detailed studies on the polymerization characteristics and kinetics, elementary reactions, characterization and behavior of the isolated key intermediates, as well as temperature and Lewis acid effects, we proposed a mechanism, outlined in Scheme 5, for the DIPP of MMA by the **1**/2Al(C_6F_5)$_3$ system. Specifically, this mechanism consists of four manifolds: isospecific, syn-

Scheme 5

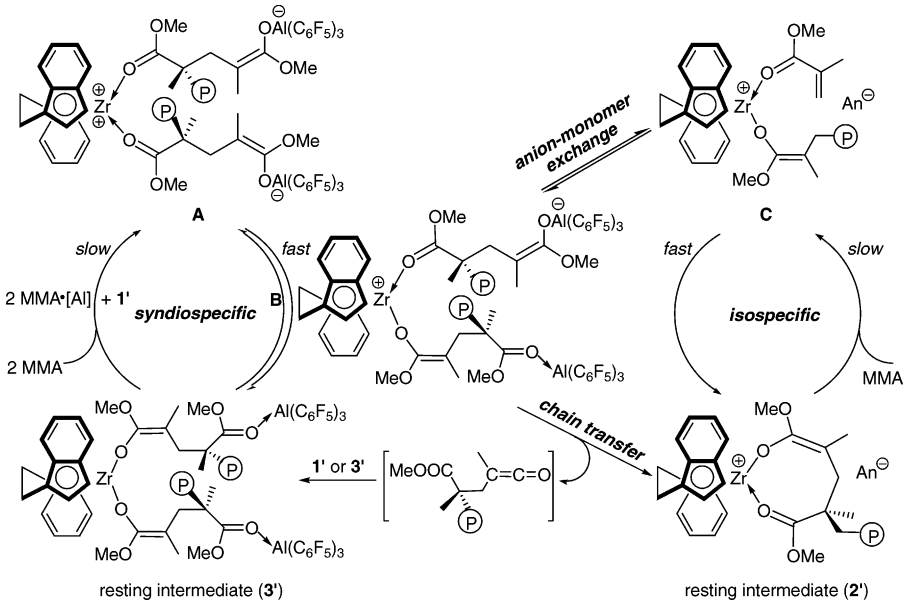

Scheme 6

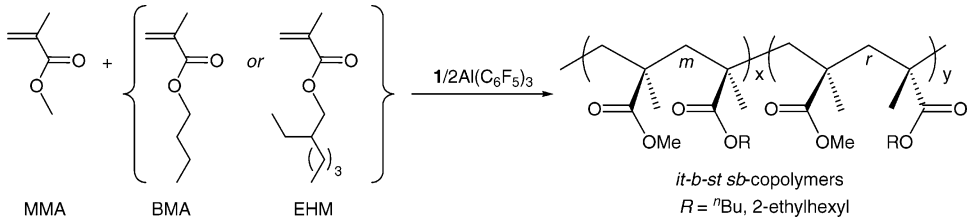

diospecific, anion−monomer exchange, and chain-transfer domains. In the *st*-block production manifold, the rate-limiting step of the bimetallic propagation involves intermolecular Michael addition of the bis(ester enolate) ligands in **1′** (**1** and its homologues) to the activated monomer MMA·Al(C_6F_5)$_3$; the resulting dicationic species **A** rapidly isomerizes to either monocationic species **B** or neutral bis(ester enolate) **3′** (**3** and its homologues) in which the coordinated alane catalyst is released by the incoming monomer to complete a *st*-P(MMA) production cycle, following the kinetics of zero order in [MMA] and second order in [Al] (cf. Schemes 1 and 2). In the isotactic block production manifold, the rate-limiting step is the associative displacement of the coordinated penultimate ester group of the growing chain in the cationic cyclic ester enolate **2′** (**2** and its homologues) by the incoming monomer to regenerate the active species **C** that participates in the fast propagating steps via intramolecular Michael addition, following first-order kinetics in [MMA]; this propagation cycle and kinetics are identical to what have been demonstrated for the MMA polymerization by the same cation but paired with the methyl borate anion.[2b]

There are two apparent pathways to interconvert two diastereospecific propagating manifolds. The first is the anion−monomer exchange process through monocationic species **B** in which the enolaluminate anion is displaced by MMA to form active species **C**, providing direct interconversion between active species **A** and **C**. The second is the chain transfer going from the resting state **3′** to **2′** also through **B** but with concomitant release of a ketene-terminated polymer chain (cf. Scheme 3) which could be instantaneously trapped by the enolate moieties present in the system (e.g., **1′** or **3′**) to regenerate a (ketone) enolate; the contribution of this chain-transfer process may be minimal under the current conditions, but its role cannot be ruled out because of the independently observed conversion of **3** to **2** within the polymerization time scale (vide supra). The high catalyst concentration regime, for example, $[MMA]_0/[Al]_0/[\mathbf{1}]_0 = 600/2/1$, favors the bimetallic, syndiotactic manifold, producing predominately *st*-P(MMA). Conversely, the low catalyst concentration regime, for example, $[MMA]_0/[Al]_0/[\mathbf{1}]_0 = 1500/2/1$, favors the monometallic, isotactic manifold, producing predominately *it*-P(MMA). The middle concentration regime with the $[MMA]_0/[Al]_0/[\mathbf{1}]_0$ ratio from 800/2/1 to 1200/2/1 affords *it-b-st* multiblock P(MMA) with various amounts of *it* and *st* contents that are a function of relative rates of interconversion vs propagation of the two diastereospecific propagating species; the rate of interconversion is regulated by the anion−monomer exchange and chain-transfer processes.

A check of the kinetic competence of the isolated two key resting intermediates has also been carried out. As expected, the MMA polymerization by **2** alone indeed produces only *it*-P(MMA), and the result of the MMA polymerization by **3** hinges on its concentration and thus the $[MMA]_0/[\mathbf{3}]_0$ ratio; in a low ratio of 400, predominately *st*-P(MMA) was produced with [*rr*] = 70.2%, [*mr*] = 22.7%, and [*mm*] = 7.1%, but in a higher ratio of 800, *it-b-st* multiblock P(MMA) was produced with [*mr*] = 18.0% and approximately equal amounts of [*rr*] and [*mm*] tacticities. These results are nearly identical to those derived from the polymerization by the **1**/2Al(C_6F_5)$_3$ system. Overall, these experimental observations and those discussed in the previous sections concerning the polymerization by the **1**/2Al-(C_6F_5)$_3$ system are consistent with the mechanism depicted in Scheme 5.

Application to Copolymerization. Homopolymers of MMA are glassy materials with a wide range of the above-ambient-temperature T_g values as a function of stereomicrostructures: *it*, ∼50 °C; *it-b-st*, ∼90 °C; *at*, ∼105 °C; *st*, ∼130 °C. To extend

Table 4. Alkyl Methacrylate Polymerization and Copolymerization Results by the 1/2Al(C_6F_5)$_3$ System [a]

run no.	monomer (comonomer)	$[M]_0/[\mathbf{1}]_0$	time (h)	conv (%)	$10^4 M_n$[b] (g/mol)	PDI[b] (M_w/M_n)	[*mm*][c] (%)	[*mr*] (%)	[*rr*] (%)	T_g (°C)
1	BMA	800	2	96	5.25	1.36	39.5	6.6	53.9	−7
2	BMA	1200	3	94	18.9	1.44	88.2	3.9	7.9	−14
3	BMA(MMA)	800	1.3	95	4.72	1.21	44.8	12.8	42.4	37
4	BMA(MMA)	1200	3	95	12.2	1.35	79.1	6.0	15.0	19
5	EHM	800	2	98	9.12	1.59	78.3	5.9	15.8	−26
6	EHM	1200	4	98	20.7	1.37	86.1	0.0	13.9	−29
7	EHM(MMA)	800	1.4	99	5.61	1.31	35.6	13.1	51.3	20
8	EHM(MMA)	1200	3.7	94	11.3	1.42	81.4	8.0	11.6	−3

[a] See Table 1 footnotes for explanations of the abbreviations listed in this table; [**1**] = 1.17 and 0.78 mM for $[monomer]_0/[\mathbf{1}]_0$ = 800 and 1200, respectively; for all copolymerizations, the monomer molar feed ratio = 1:1; 10 mL of CH_2Cl_2, 22 °C.

the utility of the above demonstrated DIPP process by the **1**/2Al(C_6F_5)$_3$ system to the production of functionalized elastomeric materials with low T_g's, we also examined its polymerizations of methacrylates with longer alkyl chains, such as *n*-butyl methacrylate (BMA) and 2-ethylhexyl methacrylate (EHM), as well as copolymerizations of MMA with BMA and EHM. Investigation into the ability of the **1**/2Al(C_6F_5)$_3$ system to produce *sb*-structures of these longer-chain alkyl methacrylate homopolymers, especially their *sb*-copolymers with MMA, is of great interest as the programmable stereomicrostructures should lead to tunable materials physical and mechanical properties of these homopolymers and *sb*-copolymers, the latter of which can potentially offer a combination of materials properties unobtainable from homopolymer blends or stereorandom copolymers.

Polymerization of BMA in a $[BMA]_0/[Al]_0/[\mathbf{1}]_0$ ratio of 800/2/1 in CH_2Cl_2 at ambient temperature produces P(BMA) with a T_g of −7 °C and a triad distribution of [*rr*] = 53.9%, [*mr*] = 6.6%, and [*mm*] = 39.5% (run 1, Table 4), consistent with the *it-b-st* multiblock microstructure. The considerably lower *ht* content of only 6.6%, compared to a typical value of [*mr*] = 16% of P(MMA) produced under identical condition, shows much longer diastereo-blocks in the resulting P(BMA), with an average *it* sequence $N_m \sim 13$ and *st* sequence $N_r \sim 17$, estimated using $N_m = 1 + 2[mm]/[mr]$ and $N_r = 1 + 2[rr]/[mr]$.[16a] As in the MMA polymerization with this ratio, the M_n of P(BMA) is consistent with the production of two polymer chains per Zr center, and increasing the ratio to 1200 yields the polymer with predominately *it* frequency [*mm*] = 88.2% and a T_g of −14 °C (run 2, Table 4). Copolymerization of BMA with MMA shows the same characteristics, producing *it-b-st sb*-copolymers (Scheme 6) with either nearly equal *it* and *st* sequences (runs 3) or predominant *it* sequences (run 4), depending on the monomer/catalyst ratio employed. The 1:1 molar composition of the two monomer units measured in the copolymers produced is identical to the monomer feed ratio, and the T_g values of the copolymer are consistent with their stereomicrostructures.

Polymerizations of EHM (runs 5 and 6) and its copolymerizations with MMA (runs 7 and 8) are similarly successful, producing *sb*-polymers and copolymers with T_g's varying from −29 to 20 °C, depending on the stereomicrostructure and comonomer. With these successful polymerization and copolymerization examples using long-chain alkyl methacrylates, it is envisioned that copolymerizations of MMA with methacrylates with even longer alkyl chains, such as octadecyl methacrylate (its homopolymer has a T_g of about −100 °C), can further lower T_g of the resulting polymer products for targeted elastomeric applications. Overall, these studies demonstrate the ability of the current DIPP system to extend its application to polymerization and copolymerization of long-chain alkyl methacrylates, thereby providing an access to fine-tune the thermal properties of the resulting functionalized polymers by regulating the stereomicrostructure of the polymer and the nature of comonomer.

Conclusions

We have demonstrated that the catalytic system comprising the readily available chiral zirconocene bis(ester enolate) *rac*-(EBI)Zr[OC(O^{i}Pr)=CMe$_2$]$_2$ (**1**) and 2 equiv of the Lewis acid Al(C_6F_5)$_3$ effectively promotes the novel diastereospecific ion-pairing polymerization (DIPP) as well as copolymerization of functionalized alkenes such as methacrylates, producing polymers having a range of stereoregularities, including *it*, *st*, and *it-b-st* multiblock microstructures, depending on the [monomer]/[catalyst] ratio employed. Our detailed investigations into the polymerization characteristics and kinetics, elementary reactions, characterization and behavior of the isolated key intermediates, temperature and Lewis acid effects, as well as applications to copolymerization have yielded a mechanism for the DIPP of MMA by the **1**/2Al(C_6F_5)$_3$ system, which consists of isospecific, syndiospecific, anion−monomer exchange, and chain-transfer manifolds. This mechanism satisfactorily explains the formation of various polymer stereomicrostructures under given conditions and reveals two pathways to interconvert diastereospecific propagating manifolds—anion−monomer exchange and chain transfer (see Scheme 5)—for the production of the multi-*it-b-st sb*-structures. From a broader perspective, this DIPP system presents unique cation−anion cooperativity in ion-pairing catalysis that involves participation from both the cation and the anion as catalysts for the same reaction, with each bringing different reactivity and stereoselectivity to the products.

The current DIPP system also presents at least two potentially significant advantages over other polymerization systems from a practical, industrial point of view. First, there is practically no need to remove inhibitors typically present in the functionalized vinyl monomers by distillation or other techniques, as required for processes such as radical polymerization. (Although the results reported in the current study were derived from the experiments employing stringently purified monomers for obvious reasons of eliminating any possible effects of other reagents on our system, selected separate experiments using the commercial-grade MMA, i.e., simple storage over molecular sieves without removal of the inhibitor, showed that the polymerization activity was not noticeably affected.) Second, the DIPP system is a simple process, but it can offer diverse polymer products having various stereomicrostructures, namely the industrially desirable approach—one catalyst system, multiple materials.

Acknowledgment. Funding for this work was provided by the National Science Foundation and Colorado State University. We thank Boulder Scientific Co. for the gift of B(C_6F_5)$_3$.

CDV

Supporting Information Available: Crystallographic data for **2**. This material is available free of charge via the Internet at http://pubs.acs.org.

References and Notes

(1) For selected recent examples and reviews, see: (a) Arriola, D. J.; Carnahan, E. M.; Hustad, P. D.; Kuhlman, R. L.; Wenzel, T. T. *Science* **2006**, *312*, 714−719. (b) Gibson, V. C.; Spitzmesser, S. K. *Chem. Rev.* **2003**, *103*, 283−315. (c) Coates, G. W.; Hustad, P. D.; Reinartz, S. *Angew. Chem., Int. Ed.* **2002**, *41*, 2236−2257. (d) Chum, P. S.; Kruper, W. J.; Guest, M. J. *Adv. Mater.* **2000**, *12*, 1759−1767. (e) Gladysz, J. A., Ed.; *Chem. Rev.* **2000**, *100*, 1167−1681 (special issue on Frontiers in Metal-Catalyzed Polymerization).

(2) (a) Rodriguez-Delgado, A.; Mariott, W. R.; Chen, E. Y.-X. *J. Organomet. Chem.* **2006**, *691*, 3490−3497. (b) Rodriguez-Delgado, A.; Chen, E. Y.-X. *Macromolecules* **2005**, *38*, 2587−2594. (c) Kostakis, K.; Mourmouris, S.; Kotakis, K.; Nikogeorgos, N.; Pitsikalis, M.; Hadjichristidis, N. *J. Polym. Sci., Part A: Polym. Chem.* **2005**, *43*, 3305−3314. (d) Ning, Y.; Cooney, M. J.; Chen, E. Y.-X. *J. Organomet. Chem.* **2005**, *690*, 6263−6270. (e) Lian, B.; Lehmann, C. W.; Navarro, C.; Carpentier, J.-F. *Organometallics* **2005**, *24*, 2466−2472. (f) Bolig, A. D.; Chen, E. Y.-X. *J. Am. Chem. Soc.* **2004**, *126*, 4897−4906. (g) Stojcevic, G.; Kim, H.; Taylor, N. J.; Marder, T. B.; Collins, S. *Angew. Chem., Int. Ed.* **2004**, *43*, 5523−5526. (h) Strauch, J. W.; Fauré, J.-L.; Bredeau, S.; Wang, C.; Kehr, G.; Fröhlich, R.; Luftmann, H.; Erker, G. *J. Am. Chem. Soc.* **2004**, *126*, 2089−2104. (i) Chen, E. Y.-X. *J. Polym. Sci., Part A: Polym. Chem.* **2004**, *42*, 3395−3403. (j) Karanikolopoulos, G.; Batis, C.; Pitsikalis, M.; Hadjichristidis, N. *J. Polym. Sci., Part A: Polym. Chem.* **2004**, *42*, 3761−3774. (k) Ferenz, M.; Bandermann, F.; Sustmann, R.; Sicking, W. *Macromol. Chem. Phys.* **2004**, *205*, 1196−1205. (l) Rodriguez-Delgado, A.; Mariott, W. R.; Chen, E. Y.-X. *Macromolecules* **2004**, *37*, 3092−3100. (m) Jensen, T. R.; Yoon, S. C.; Dash, A. K.; Luo, L.; Marks, T. J. *J. Am. Chem. Soc.* **2003**, *125*, 14482−14494. (n) Chen, E. Y.-X.; Cooney, M. J. *J. Am. Chem. Soc.* **2003**, *125*, 7150−7151. (o) Mariott, W. R. Chen, E. Y.-X. *J. Am. Chem. Soc.* **2003**, *125*, 15726−15727. (p) Jin, J.; Mariott, W. R.; Chen, E. Y.-X. *J. Polym. Chem. Part A: Polym. Chem.* **2003**, *41*, 3132−3142. (q) Batis, C.; Karanikolopoulos, G.; Batis, C.; Pitsikalis, M.; Hadjichristidis, N. *Macromolecules* **2003**, *36*, 9763−9774. (r) Karanikolopoulos, G.; Batis, C.; Pitsikalis, M.; Hadjichristidis, N. *Macromol. Chem. Phys.* **2003**, *204*, 831−840. (s) Bolig, A. D.; Chen, E. Y.-X. *J. Am. Chem. Soc.* **2002**, *124*, 5612−5613. (t) Jin, J.; Chen, E. Y.-X. *Organometallics* **2002**, *21*, 13−15 (u) Bandermann, F.; Ferenz, M.; Sustmann, R.; Sicking, W. *Macromol. Symp.* **2001**, *174*, 247−253. (v) Karanikolopoulos, G.; Batis, C.; Pitsikalis, M.; Hadjichristidis, N. *Macromolecules* **2001**, *34*, 4697−4705. (w) Bolig, A. D.; Chen, E. Y.-X. *J. Am. Chem. Soc.* **2001**, *123*, 7943−7944. (x) Frauenrath, H.; Keul, H.; Höcker, H. *Macromolecules* **2001**, *34*, 14−19. (y) Nguyen, H.; Jarvis, A. P.; Lesley, M. J. G.; Kelly, W. M.; Reddy, S. S.; Taylor, N. J.; Collins, S. *Macromolecules* **2000**, *33*, 1508−1510. (z) Bandermann, F.; Ferenz, M.; Sustmann, R.; Sicking, W. *Macromol. Symp.* **2000**, *161*, 127−134. (aa) Cameron, P. A.; Gibson, V.; Graham, A. J. *Macromolecules* **2000**, *33*, 4329−4335. (bb) Stuhldreier, T.; Keul, H.; Höcker, H. *Macromol. Rapid Commun.* **2000**, *21*, 1093−1098. (cc) Chen, Y.-X.; Metz, M. V.; Li, L.; Stern, C. L.; Marks, T. J. *J. Am. Chem. Soc.* **1998**, *120*, 6287−6305. (dd) Shiono, T.; Saito, T.; Saegusa, N.; Hagihara, H.; Ikeda, T.; Deng, H.; Soga, K. *Macromol. Chem. Phys.* **1998**, *199*, 1573−1579. (ee) Li, Y.; Ward, D. G.; Reddy, S. S.; Collins, S. *Macromolecules* **1997**, *30*, 1875−1883. (ff) Deng, H.; Shiono, T.; Soga, K. *Macromol. Chem. Phys.* **1995**, *196*, 1971−1980. (gg) Deng, H.; Shiono, T.; Soga, K. *Macromolecules* **1995**, *28*, 3067−3073. (hh) Soga, K.; Deng, H.; Yano, T.; Shiono, T. *Macromolecules* **1994**, *27*, 7938−7940. (ii) Collins, S.; Ward, D. G.; Suddaby, K. H. *Macromolecules* **1994**, *27*, 7222−7224. (jj) Collins, S.; Ward, S. G. *J. Am. Chem. Soc.* **1992**, *114*, 5460−5462. (kk) Farnham, W. B.; Hertler, W. U.S. Pat. 4,728,706, 1988.

(3) (a) Mariott, W. R.; Rodriguez-Delgado, A.; Chen, E. Y.-X. *Macromolecules* **2006**, *39*, 1318−1327. (b) Kostakis, K.; Mourmouris, S.; Pitsikalis, M.; Hadjichristidis, N. *J. Polym. Sci., Part A: Polym. Chem.* **2005**, *43*, 3337−3348. (c) See ref 2ee. (d) Deng, H.; Soga, K. *Macromolecules* **1996**, *29*, 1847−1848.

(4) (a) Mariott, W. R.; Chen, E. Y.-X. *Macromolecules* **2005**, *38*, 6822−6832. (b) Mariott, W. R.; Chen, E. Y.-X. *Macromolecules* **2004**, *37*, 4741−4743.

(5) Hatada, K.; Kitayama, T.; Ute, K. *Prog. Polym. Sci.* **1988**, *13*, 189−276.

(6) (a) Harney, M. B.; Zhang, Y.; Sita, L. R. *Angew. Chem., Int. Ed.* **2006**, *45*, 1−5. (b) Coates, G. W.; Waymouth, R. M. *Science* **1995**, *267*, 217−219. (c) Llinas, G. L.; Dong, S.-H.; Mallin, D. T.; Rausch, M. D.; Lin, G.-Y.; Winter, H. H.; Chien, J. C. W. *Macromolecules* **1992**, *25*, 1242−1253.

(7) (a) Serizawa, T.; Hamada, K.-I.; Akashi, M. *Nature (London)* **2004**, *429*, 52−55. (b) Serizawa, T.; Hamada, K.; Kitayama, T.; Fujimoto, N.; Hatada, K.; Akashi, M. *J. Am. Chem. Soc.* **2000**, *122*, 1891−1899. (c) Hatada, K.; Kitayama, T.; Ute, K.; Nishiura, T. *Macromol. Symp.* **1998**, *132*, 221−230. (d) Spevacek, J.; Schneider, B. *Adv. Colloid Interface Sci.* **1987**, *27*, 81−150.

(8) (a) See refs 2n and 2s. (b) Knjazhanski, S. Y.; Elizalde, L.; Cadenas, G.; Bulychev, B. M. *J. Polym. Sci., Part A: Polym. Chem.* **1998**, *36*, 1599−1606. (c) Kitayama, T.; Fujimoto, N.; Yanagida, T.; Hatada, K. *Polym. Int.* **1994**, *33*, 165−170.

(9) Allen, R. D.; Long, T. E.; McGrath, J. E. *Polym. Bull. (Berlin)* **1986**, *15*, 127−134.

(10) Feng, S.; Roof, G. R.; Chen, E. Y.-X. *Organometallics* **2002**, *21*, 832−839.

(11) (a) Lee, C. H.; Lee, S. J.; Park, J. W.; Kim, K. H.; Lee, B. Y.; Oh, J. S. *J. Mol. Catal., A: Chem.* **1998**, *132*, 231−239. (b) Biagini, P.; Lugli, G.; Abis, L.; Andreussi, P. U.S. Pat. 5,602269, 1997.

(12) Shreve, A. P.; Mulhaupt, R.; Fultz, W.; Calabrese, J.; Robbins, W.; Ittel, S. *Organometallics* **1988**, *7*, 409−416.

(13) (a) Grossman, R. B.; Doyle, R. A.; Buchwald, S. L. *Organometallics* **1991**, *10*, 1501−1505. (b) Collins, S.; Kuntz, B. A.; Taylor, N. J.; Ward, D. G. *J. Organomet. Chem.* **1988**, *342*, 21−29.

(14) Diamond, G. M.; Jordan, R. F.; Petersen, J. L. *J. Am. Chem. Soc.* **1996**, *118*, 8024−8033.

(15) Rodriguez-Delgado, A.; Chen, E. Y.-X. *J. Am. Chem. Soc.* **2005**, *127*, 961−974.

(16) (a) Bovey, F. A.; Mirau, P. A. *NMR of Polymers*; Academic Press: San Diego, CA, 1996. (a) Bulai, A.; Jimeno, M. L.; de Queiroz, A.-A. A.; Gallardo, A.; Roman, J. S. *Macromolecules* **1996**, *29*, 3240−3246. (c) Ferguson, R. C.; Ovenall, D. W. *Macromolecules* **1987**, *20*, 1245−1248. (d) Subramanian, R.; Allen, R. D.; McGrath, J. E.; Ward, T. C. *Polym. Prepr.* **1985**, *26*, 238−240.

(17) *SHELXTL*, Version 6.12; Bruker Analytical X-ray Solutions: Madison, WI, 2001.

(18) Chakraborty, D.; Chen, E. Y.-X. *Inorg. Chem. Commun.* **2002**, *5*, 698−701.

(19) (a) Yasuda, H.; Yamamoto, H.; Yamashita, M.; Yokota, K.; Nakamura, A.; Miyake, S.; Kai, Y.; Kanehisa, N. *Macromolecules* **1993**, *26*, 7134−7143. (b) Yasuda, H.; Yamamoto, H.; Yokota, K.; Miyake, S.; Nakamura, A. *J. Am. Chem. Soc.* **1992**, *114*, 4908−4909.

(20) (a) Stahl, N. G.; Salata, M. R.; Marks, T. J. *J. Am. Chem. Soc.* **2005**, *127*, 10898−10909. (b) Chen, E. Y.-X.; Kruper, W. J.; Roof, G.; Wilson, D. R. *J. Am. Chem. Soc.* **2001**, *123*, 745−746. (c) Liu, Z.; Somsook, E.; Landis, C. R. *J. Am. Chem. Soc.* **2001**, *123*, 2915−2916.

(21) Spaether, W.; Klass, K.; Erker, G.; Zippel, F.; Fröhlich, R. *Chem.−Eur. J.* **1998**, *4*, 1411−1417.

MA061687W